Yield stress and wall slip phenomena in colloidal silica gels

H. J. Walls,[a] S. Brett Caines, Angelica M. Sanchez, and Saad A. Khan[b]

Department of Chemical Engineering, North Carolina State University, Raleigh, North Carolina 27695-7905

(Received 22 July 2002; final revision received 21 February 2003)

Synopsis

Evidence of wall slip and magnitude of yield stress are examined for colloidal gels consisting of hydrophobic silica, polyether, and lithium salts using geometries with serrated, smooth, hydrophilic and hydrophobic surfaces. Serrated plates, which provide minimal wall slip, are used to compare different methods of measuring yield stress: conventional extrapolation of shear stress in steady shear experiments and dynamic experiments at large strain amplitudes. In the latter, the yield stress is denoted by the maximum in the elastic stress, the product of the elastic modulus and strain ($G'\gamma$), when plotted as a function of strain amplitude. Although excellent agreement is observed in the yield stress values using both these techniques, the dynamic method seems preferable considering its experimental ease, accuracy, and lack of extrapolation. In the presence of smooth geometries, the silica gels show evidence of wall slip with a concomitant decrease in yield stress. Using underestimation of yield stress as a measure of wall slip, we find slip to be unaffected by changes in the gel modulus obtained through incorporation of additional silica or salts. The use of smooth surfaces compared to serrated surfaces leads to approximately a 60% reduction in yield stress for all such samples. Finally, control of wall slip is attempted using plates modified to have different surface energies. Hydrophobic plates reduce slip significantly and produce data comparable to those with the serrated plates. In contrast, hydrophilic plates have minimal effect on slip and produce data analogous to those obtained using smooth plates. These results can be explained based on the fact that the particle-lean layer, responsible for slip, remains so with hydrophilic plates as it repels the hydrophobic silica particles in favor of the polar solvent. In contrast, the hydrophobic silica interacts with the hydrophobic plates, thus reducing slip. [DOI: 10.1122/1.1574023]

I. INTRODUCTION

An extensive array of complex materials, ranging from consumer products such as paints and mayonnaise to advanced materials such as insulating gels for fiber-optic cables and electrolytes for new generation batteries, exhibit yield stress. Despite its obvious importance, however, yield stress remains a topic of controversy and experimental frustration [Nguyen and Boger (1983); Yoshimura *et al.* (1987); Evans (1992); Nguyen and Boger (1992); Husband and Aksel (1993); Macosko (1994); Barnes (1995, 1999); Roberts and Barnes (2001)]. Particulate and colloidal suspensions have proved particularly difficult systems in which to study yield stress due to the occurrence of wall slip and the

[a]Current address: Polymers Division, National Institute of Standards and Technology, Gaithersburg, MD 20899-8542

[b]Author to whom all correspondence should be addressed; electronic mail: khan@eos.ncsu.edu

history-dependent microstructures that form, giving rise to different values of apparent yield stresses [Buscall *et al.* (1993); Aral and Kalyon (1994); Soltani and Yilmazer (1998); Barnes (1999); Russel and Grant (2000)].

In this study, we explore the measurement of yield stress and the occurrence of slip in colloidal silica gels. These gels are composed of fumed silica particulates dispersed in oligomers of poly(ethylene oxide) containing lithium salts. In its native form, fumed silica consists of silicon dioxide particles fused together to form a submicron, branched structure. The surface is hydrophilic and consists of silanol groups; however, the silanol groups can be replaced by other moieties that allow a wide range of surface characteristics. These unique materials have numerous applications including coatings, paints, membranes, and composite electrolytes [Raghavan *et al.* (1998); Walls *et al.* (2000)]. Considerable work has therefore been undertaken in understanding the rheology of these systems, particularly in terms of the colloidal interactions and shear induced changes in microstructure [Raghavan and Khan (1995); Raghavan *et al.* (1998, 2000); Walls (2002)]. However, very little effort has been made in examining its yield stress and wall-slip characteristics, both of which are important from academic and industrial standpoints.

In this study, we use fumed silica that has octyl chains tethered to its surface, thus rendering it hydrophobic. When a sufficient amount of this fumed silica is dispersed in a polar medium, an interconnecting network forms, producing a physical gel. For lithium battery applications, researchers are interested in polymers that solvate a lithium salt and form a chemically stable interface with lithium metal. Poly(ethylene oxide) (PEO) and poly(propylene oxide) (PPO) have become choice polymers for the study of polymer electrolytes for batteries [Gray (1997)]. We have chosen to focus on oligomers of PEO because of their superior room temperature conductivities [Shi and Vincent (1993); Fan *et al.* (1998)].

A. Wall slip

The causes of wall slip, its detection, and correction, as well as methods for estimating the yield stress in suspensions and colloidal gels have been investigated by a variety of researchers [Yang *et al.* (1986); Yoshimura *et al.* (1987); Buscall *et al.* (1993); Aral and Kalyon (1994); Soltani and Yilmazer (1998); Shih *et al.* (1999); Yziquel *et al.* (1999); Russel and Grant (2000); Gevgilili and Kalyon (2001)]. In colloidal and other suspensions, the general belief is that a thin layer of fluid exists next to the test geometry (the wall) with the particles either not interacting with the wall or interacting weakly. At sufficiently high shear rates, the velocity of the fluid next to the wall is higher than that of the bulk material. In the extreme case, the particle-lean fluid near the wall flows, while the bulk material does not deform at all. Polymer melts are also capable of exhibiting wall slip [Hatzikiriakos and Dealy (1991); Macosko (1994)]. For polymer melts, the theories focus on the formation of a lubrication layer at the wall, or on the polymer bonding and debonding with the surface [Macosko (1994); Leger *et al.* (1997); Anastasiadis and Hatzikiriakos (1998); Joshi *et al.* (2000)]. In both suspensions and polymer melts, the bulk material deforms less than the layer close to the wall. However, in colloids a discontinuous system is expected where the sample composition near the wall is different than the bulk composition.

One of the accepted ways by which to detect wall slip is to make steady shear measurements of the same sample material for two largely different gap sizes either in parallel plate or couette geometry. Yoshimura *et al.* (1987) developed a mathematical treatment for wall-slip correction using steady shear data taken at two different gap sizes. They were able to produce corrected stress versus shear rate curves and estimate slip velocities for dilute bentonite suspensions in water and oil in water emulsions. Russel and

Grant (2000) developed a model for slip in colloidal silica suspensions. Their model suggests the occurrence of a Newtonian plateau at low shear stresses in a plot of viscosity versus shear stress. Russel and Grant (2000) found that varying the gap size with parallel plates did not produce large enough differences for their colloidal gels to determine slip velocities due to the uncertainty of the measurement.

Perhaps the best methods of dealing with slip in suspensions are to use vane geometry or geometries with roughened surfaces [Nguyen and Boger (1983); Yoshimura *et al.* (1987); Buscall *et al.* (1993); Barnes and Nguyen (2001)]. Although the vane geometry is popular in the study of concentrated suspensions because it effectively eliminates slip, it requires a much larger sample volume than the parallel plate geometry. In this regard, roughened parallel plates obtained through attachment of sandpaper or treatment with sand blasting, or commercially available serrated plates with ridges, have found extensive use in eliminating slip. Buscall *et al.* (1993) compared viscosity as a function of shear stress for a flocculated suspension of an acrylic copolymer in poly(isobutylene) for couette geometries with smooth and roughened surfaces. The smooth geometries showed much lower yield stress and exhibited a low-stress Newtonian plateau in a viscosity versus shear stress plot. At high shear stresses the flow curves of both smooth and roughened geometries converged. The occurrence of a low-stress plateau in a plot of viscosity versus shear stress has been observed in a variety of gel materials when slip is present [Buscall *et al.* (1993); Barnes (1995); Russel and Grant (2000); Roberts and Barnes (2001)].

B. Yield stress

Although wall slip is one of the major confounding factors in estimating yield stress, reproducible measurement of yield stress in gel materials can be challenging even after wall slip is eliminated. Barnes (1995, 1999) gave an extensive review of determining yield stress that focused on the differences amongst various techniques. A number of researchers have conducted comparative studies of yield stress measurement using techniques from steady shear rheology and creep on systems ranging from latexes and clay suspensions to yogurt [Nguyen and Boger (1983); Yoshimura *et al.* (1987); Buscall *et al.* (1993); Husband and Aksel (1993); Dimonte *et al.* (1998)]. The majority of the techniques use steady shear stress or rate (as opposed to dynamic or oscillatory) experiments. The data are plotted as apparent viscosity versus shear stress or as shear stress versus the rate. For a viscosity plot, the viscosity exhibits a rapid decrease with an increase in shear above the yield stress. The yield stress, then, is estimated as the stress at which viscosity just starts to exhibit a rapid drop in value. For plots of shear stress versus the rate, two approaches to data analysis are taken. The first is to use a linear plot and fit the data to one of several models that contain a yield stress parameter, such as the classic Bingham model [Macosko (1994)]. However, fitting the data to a yield stress model can lead to overestimation of the yield stress and not all materials comply with common yield stress models [Barnes (1999); Barnes and Nguyen (2001)]. The second approach is to use a log plot which typically shows Newtonian behavior at very high shear rates and ''stress plateaus'' at low stresses [Yang *et al.* (1986); Evans (1992)]. The stress plateaus are then taken as the yield stress. In all cases of the steady stress measurements discussed, it is a challenge to find the point of largest applied shear stress before material flow occurs. One confounding problem is the very large uncertainties that are observed at shear stresses and shear rates below the apparent yield stress.

In a vane geometry measurement, a cylinder with a number of thin blades is immersed in the sample and shear stress is monitored versus time in a steady rotation experiment.

The maximum in shear stress with respect to time is interpreted as the yield stress. One drawback of the vane method is the aforementioned large sample size required. Another problem that can occur with the vane geometry method is that in some cases the observed yield stress depends on the rate of rotation [Nguyen and Boger (1983)].

Creep and tensile creep measurements have received attention as another way of estimating yield stress [Husband and Aksel (1993)]. In creep experiments, a sample is subjected to constant stress over a long period of time and the resulting strain is monitored. Below the yield stress the sample responds to the applied stress by approaching a constant strain value. Above the yield stress, the strain increases rapidly and achieves a constant slope in a plot of strain versus time. The drawback to this technique is that a series of time-consuming measurements are needed and it is helpful to have an estimate of the yield stress before beginning the experiments.

An alternative to steady shear rate and creep tests is the use of oscillatory or dynamic strain or shear stress measurements. Dynamic experiments for estimation of yield stresses have been used considerably less than steady tests, perhaps because they are biased by the notion that yield stress has to do with flow and hence standard flow measurements must be used to estimate yield stress. Dynamic strain data have been used to estimate the yield stress of iron oxide suspensions in silicone oil and compared against that obtained by steady stress tests [Yang *et al.* (1986)]. Yang and co-workers (1986) used a dynamic strain sweep at a frequency of 0.1 rad/s and replotted the data as the product of the elastic modulus and absolute strain amplitude (we shall refer to this as the elastic stress) versus strain. A maximum in the elastic stress curve is interpreted as the yield stress. Yang *et al.* found good agreement with constant shear data and dynamic strain data in estimating the yield stress of their materials. Pai and Khan (2002) exploited this elastic stress method to estimate the yield stress for xanthan–guar blend gels. Shih and co-workers (1999) also used dynamic strain sweeps on boehmite gels but interpreted the crossover of G' and G'' as the yield stress of the colloidal gel.

The use of dynamic strain or stress experiments to measure yield stresses has several advantages. First, a variety of test geometries including those with roughened surfaces may be used depending upon the sample requirements. Second, dynamic rheology experiments can provide, simultaneously, information about a sample's viscoelastic properties and/or microstructure, and the yield stress. Third, *a priori* estimation of a material's yield stress is not required. Finally, reliable data are obtained both above and below the yield stress, as opposed to the large uncertainties obtained at low shear rates for the steady shear flow experiments.

In this paper, we initially compare yield stress estimation from steady shear experiments to those obtained via dynamic stress measurements. A variety of samples of interest to us are tested and compared via the use of serrated parallel plates. When geometries with smooth surfaces are used, e.g., cone and plate or parallel plates, wall slip is apparent. We examine this slip phenomenon as a function of the physical properties of the colloidal gel. In particular, the effects of gel modulus, solvent properties due to salt content, and solvent type (e.g., molecular weight and structure) are investigated. Finally, we study the effect of parallel plate surface chemistry in controlling wall slip. A thin layer of poly(dimethylsiloxane) (PDMS) is crosslinked to the surface of a pair of smooth parallel plates. The surface properties of the PDMS are then modified to give either a hydrophobic or a hydrophilic surface chemistry. The results for the two surface-modified plates were compared against those obtained with bare parallel plates and serrated plates.

TABLE I. Oligomers used in this study.

Solvating oligomer	Abbreviation	Viscosity (Pa s)	Density (g/ml)
Poly(ethylene glycol) dimethyl ether $M_n \sim 250$	PEGdm 250	0.0068	1.03
Poly(ethylene glycol) dimethyl ether $M_n \sim 500$	PEGdm 500	0.028	1.05
Tetra(ethylene glycol) M = 194.24	TEG	0.047	1.125
Poly(propylene glycol) $M_n \sim 425$	PPG 425	0.068	1.004
Poly(propylene glycol) $M_n \sim 725$	PPG 725	0.118	1.007

II. EXPERIMENTAL MATERIALS AND METHODS

A. Materials

Two types of gels were prepared, ones containing salt (electrolytic gel) and the others without any salt. The electrolyte gels were composed of lithium salt, poly(ethylene glycol) dimethyl ether, and hydrophobic fumed silica containing tethered octyl chains. Since low moisture content is important in the study of polymer electrolytes, procedures were followed to produce samples with minimal moisture content. Lithium bis(trifluoromethanesulfonyl)imide $[Li(CF_3SO_2)_2N]$ (LiTFSI, 3M Co.), was dried under vacuum at 80 °C for 48 h before use. Hydrophobic fumed silica (Aerosil R805, Degussa) was dried at 120 °C under vacuum for five days. R805 fumed silica has octyl (C_8H_{17}) groups attached to its native Si–OH surface at a surface coverage of 50% [Raghavan *et al.* (2000)]. Poly(ethylene glycol) dimethyl ether ($250\,M_n$, Aldrich) was dried over 4 Å molecular sieves for one week. All chemicals were stored and used within an argon-filled glove box (moisture content < 5 ppm).

Salt-free fumed silica gels were made using a variety of oligomers. Table I lists all the oligomers used in this study along with some of their physical properties and the abbreviation used in this study. These gels were prepared outside the glove box. The viscosities were measured using the steady shear experiments described below. The manufacturer (Aldrich) provided the densities.

B. Sample preparation

Fumed silica was dispersed into the solvating medium via a high shear mixer (Tissue-Tearor, BioSpec) with a 7 mm diam probe. The samples were then degassed under vacuum to remove entrained air bubbles. All samples were stored in a desiccator before use and discarded after 24 h to minimize aging effects due to moisture uptake.

Given that the volume fraction of filler is important in the study of colloidal gels, estimates of the density of the fumed silica and solvating medium are required. The density of the liquid electrolyte (PEGdm and salt with no fumed silica) changes with the salt concentration as shown in Fig. 1. These properties were measured in a previous study [Walls (2002)]. Based on earlier work, we use a density of 2.2 g/cm^3 for fumed silica [Khan and Zoeller (1993)]. The volume fraction of fumed silica was then estimated as the volume of fumed silica added to a volume of solvating medium, either liquid electrolyte

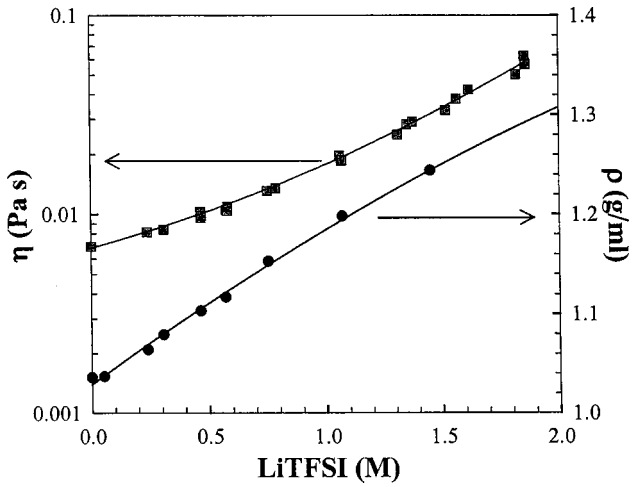

FIG. 1. Density and Newtonian viscosity of a liquid electrolyte comprised of polyethylene glycol dimethyl ether (PEGdm 250) and lithium imide (LiTFSI) salt.

as in Fig. 1 or pure oligomer as in Table I. This approach was used because determination of the actual volume fraction of the fumed silica in the final sample is inordinately difficult.

C. Rheology

Dynamic and steady rheology experiments were performed in a Rheometrics Dynamic Stress Rheometer (DSR II). Several different test geometries were used according to the sample and test requirements including (i) 40 mm cone and plate with a cone angle of 0.05 rad, (ii) 25 mm cone and plate with a cone angle of 0.1 rad, (iii) 40 and 25 mm parallel plates with ridged surfaces (serrated plates), (iv) couette, and, (v) 25 mm parallel plates coated with PDMS as detailed below.

Since sample history influences the microstructure of fumed silica [Raghavan and Khan (1995)], a meticulous routine for sample loading and delay before testing was followed to give consistent results. Freshly made samples (less than 24 h old) were first hand mixed with a spatula right before use. All samples were first tested with the cone and plate geometry. After a delay time of more than 5 min, a dynamic frequency sweep from an angular frequency (ω) of only 0.4–40 rad/s at constant stress amplitude (σ) in the range of 3.5–10 Pa was done. This short frequency range, used for all dynamic frequency tests, was chosen to conserve experimental time. Dynamic frequency tests at lower frequencies are found elsewhere and verify that these materials are true gels [Raghavan (1998); Raghavan *et al.* (2000); Walls (2002)]. A second delay time is applied and the dynamic frequency test repeated to check for reproducibility. The uncertainty of the gel modulus G', determined from the dynamic frequency test, for a single sample (whether the tests were done on the same or different aliquot of the sample) was less than 7%. These dynamic frequency tests were then used as the baseline for all subsequent tests. For example, if a steady stress test using serrated plates is to be done, first that sample is subjected to a dynamic frequency test with the serrated plates and the results referenced back to the cone and plate dynamic frequency results for that sample. Then, the steady stress test would be performed.

Typically, tests were performed as sets for a single sample composition. An aliquot of the sample would be tested with the cone and plate geometry and the aforementioned initial dynamic frequency sweeps performed. Then either a dynamic stress or steady stress test would be performed. The loaded sample would then be discarded and a new aliquot loaded and subjected to dynamic frequency tests, which are then compared with the initial tests to check that the sample was loaded correctly and that reproducibility is observed. Then, a new dynamic stress or steady stress test would be performed.

The dynamic stress experiments were done at a frequency of 1 rad/s. Steady stress measurements were performed on liquid samples (i.e., no fumed silica) with the couette geometry to determine the Newtonian viscosity and are reported in Fig. 1 or Table I. Steady stress experiments to determine yield stress were done with either 25 or 40 mm serrated plates.

D. Modification of test geometry surface energy

Parallel plate geometries with different surface energies were used in some of our studies. Surface modification was done by coating test plates with PDMS, details of which are given elsewhere [Efimenko *et al.* (2002)]. Stainless steel 25 mm parallel plates were coated with Sylgard-184 from Dow Corning. Sylgard-184 is an elastomeric poly-(dimethyl siloxane) which can be cast as a thin film and cured to form a smooth surface with an elastic modulus significantly larger ($> 100\times$) than that of the gels studied here. Samples were cured at 60 °C in a vacuum oven. The cured PDMS surface is hydrophobic. This PDMS surface can be modified to be hydrophilic via exposure to ultraviolet and ozone (UVO) [Efimenko *et al.* (2002)]. UVO treatment was carried out in a commercial UVO chamber (Jetlight Company, Inc. model 42). Once a set of hydrophobic or hydrophilic parallel plates was produced, they were stored in a clean dry environment and used within 24 h.

III. RESULTS AND DISCUSSION

A. Yield stress measurement techniques

We first compare yield stresses using serrated plates (that provide the absence of or minimal wall slip) for two different experimental methods. In the first approach, steady shear experiments are done as a function of increasing stress. Figure 2 shows data from a steady stress experiment for an electrolyte gel comprised of 1.07 M LiTFSI in PEGdm 250 with a fumed silica volume fraction (ϕ) of about 0.051. In Fig. 2(a), which plots the apparent viscosity as a function of shear stress, the yield stress corresponds to the point where the material exhibits a catastrophic drop in viscosity, indicated by the arrow. At very low shear stresses, we observe the appearance of a Newtonian plateau, which Russel and Buscall have attributed to wall slip. We believe it is unreliable data resulting from the sample not reaching steady state at such low shear rates or signals below the transducer limit of the instrument. An alternate way of examining the data in Fig. 2(a) is to plot shear stress versus the shear rate, as shown in Fig. 2(b). In this case, the yield stress corresponds to the transition point denoted in Fig. 2(b). Yang and co-workers (1986) used plots similar to that in Fig. 2(b) to estimate the yield stress of iron oxide in silicone oil suspensions. They observed a plateau in shear stress at shear rates in the 10^{-3}–$10^{-1}\,s^{-1}$ range, which they interpreted as the yield stress. We interpret the transition from very low, unreliable shear rates to measurable shear rates [indicated by the line in Fig. 2(b)] as the point of yield stress. The method we used to estimate the yield stress from steady shear data for our samples was to examine plots similar to Figs. 2(a) and 2(b) and make a set of estimates for the yield stress for each sample. This set of yield stress estimates

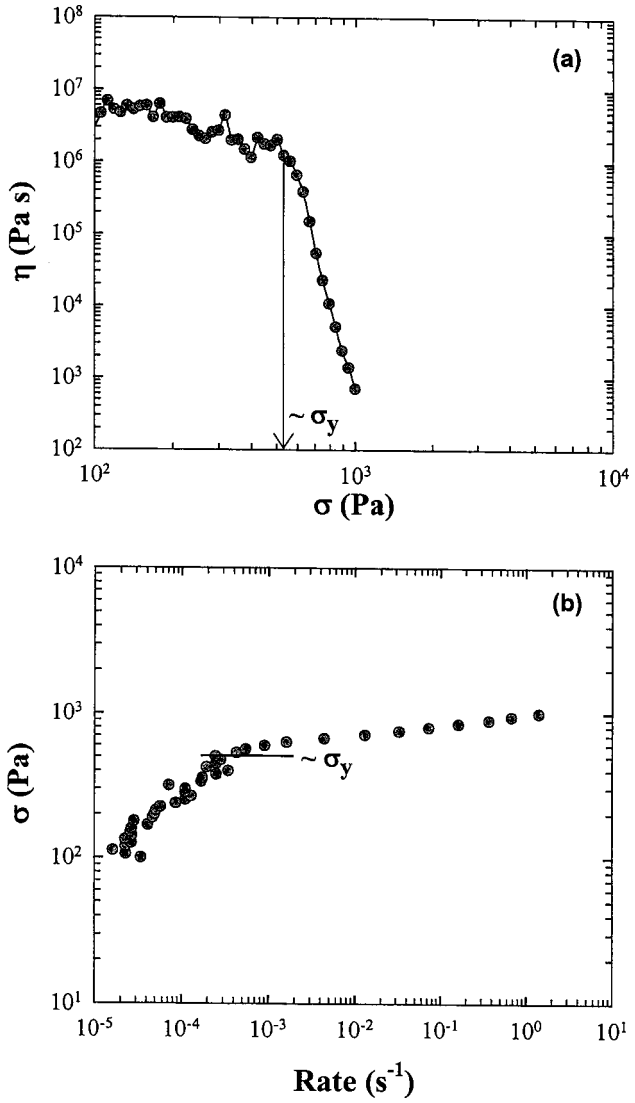

FIG. 2. Steady stress sweep data for estimating yield stress. The sample is 1.07 M LiTFSI in PEGdm 250 and fumed silica volume fraction (ϕ) $\sim$ 0.051. (a) Apparent viscosity vs shear stress. (b) Shear stress vs shear rate.

was then averaged to give the best estimate of yield stress from the steady shear data. The uncertainty in the measurement from this steady shear method was typically less than 15%.

To further test our hypothesis that the low shear rate data are a result of the measurement not reaching steady state and hence the viscosity values given are incorrect, we performed a series of creep measurements and compared them with steady stress measurement on a gel of 1.06 M LiTFSI and $\phi \sim 0.035$. The steady stress results, similar to that in Fig. 2(a), exhibited a pseudoplateau at low shear stresses (less than 100 Pa) with $\eta \sim 3 \pm 1 \times 10^6$ Pa. However, if constant stress is applied for a long period of time and the strain response monitored, much larger viscosities are observed [Walls (2002)]. For example, applied stress of 30 Pa for 20 min results in $\eta \sim 2 \times 10^7$ Pa and 30 Pa for 2 h

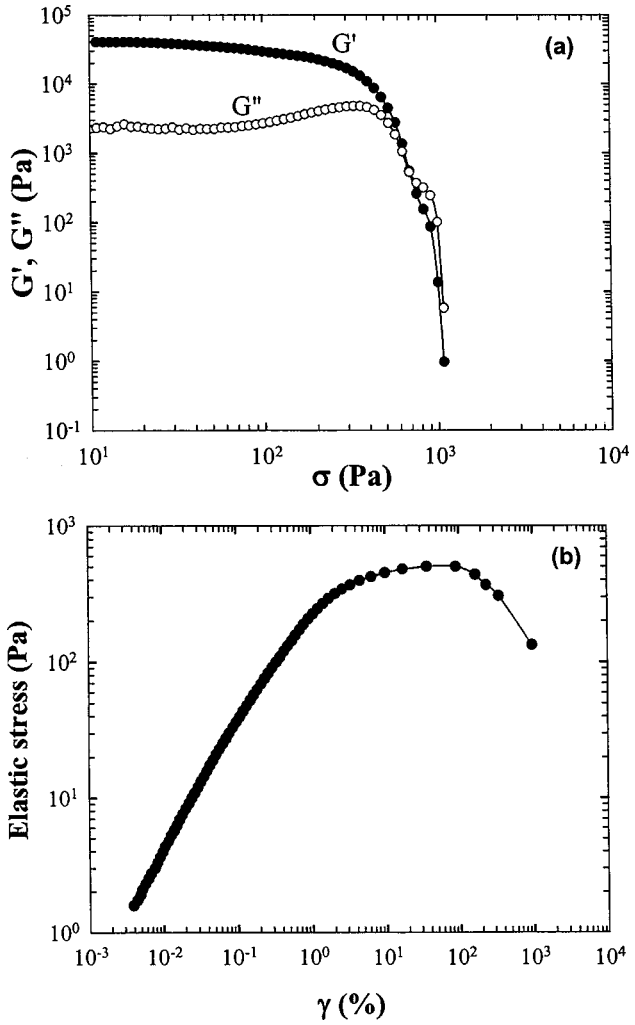

FIG. 3. Dynamic stress data for the sample in Fig. 2. (a) Dynamic stress sweep showing the fumed silica network structure rupturing at high stresses. (b) Elastic stress ($G'\gamma$) plotted as a function of the strain amplitude. The maximum in the elastic stress curve is interpreted as the yield stress of the material.

results in $\eta \sim 2\times10^8$ Pa, indicating clearly that the viscosity values at low shear rates/stresses are not at steady state.

The second experimental method of estimating the yield stress is to conduct dynamic experiments as a function of increasing stress amplitude. Figure 3(a) shows the elastic (G') and viscous (G'') moduli for the 1.07 M, $\phi \sim 0.051$ gel used in Fig. 2 as a function of increasing stress amplitude. At high shear amplitudes G' begins to decrease due to rupture of the fumed silica network and eventually crosses G''. The crossover of G' and G'' has been used as one estimate of the yield stress [Shih *et al.* (1999)]. The dynamic stress data can, however, be recast as the elastic stress (G' multiplied by absolute strain) and plotted against strain, as shown in Fig. 3(b). The maximum in the elastic stress curve is then interpreted as the yield stress [Yang *et al.* (1986)]. These two methods of estimating the yield stress are less subjective than those we used for the steady stress data.

TABLE II. Comparison of yield stress measurements for five different gel samples.

Samples [LiTFSI]; ϕ	Gel G' (Pa)	Yield stress estimate methods (Pa)		
		Steady stress	Elastic stress	G', G'' crossover
0 M; 0.0445	6.98×10^3	100	111	156
0.24 M; 0.0467	1.67×10^4	215	193	266
1.07 M; 0.0272	2.90×10^3	56	72.5	100
1.07 M; 0.0513	3.76×10^4	534	499	694
1.86 M; 0.0395	1.82×10^4	309	332	456

Table II gives a comparison of the yield stress measurement on five different samples where salt and fumed silica content were varied. The gel modulus, an average of G' from cone and plate dynamic frequency sweeps, is included for completeness. For each sample, all three methods produce similar values of the yield stress. The only exception is the 1.07 M, $\phi = 0.0272$ gel, which might be attributed to experimental error such as a sample-loading problem. However, even in this case, the estimates are all in the same range. The elastic stress method and steady shear method produce results that are within $\pm 10\%$ of each other. The G', G'' crossover method seems to consistently overestimate the yield stress by about 40%. We consider the elastic stress method to be the most preferable method of yield stress estimation, given the lack of subjectivity, the reliable and simple nature of the experiment, and its close match with conventional steady stress methods [Yang *et al.* (1986)].

One important issue to address with respect to using dynamic rheology to estimate yield stresses is the effect of frequency. We performed a series of dynamic stress measurements in which frequencies of 0.1, 1, and 5 rad/s were used. The yield stress values, given by the elastic stress method for this range of frequencies, were found to vary less than the uncertainty in the measurement. Thus, for our gels at low frequencies, estimation of the yield stress via dynamic measurements is independent of the frequency used, and is comparable to the value obtained via traditional steady stress measurements.

B. Effect of gel properties on slip

We now turn our attention to issues of slip in fumed silica gels. Figure 4 shows steady and dynamic shear data for a 1.06 M, $\phi \sim 0.045$ gel using both cone and plate and serrated plate geometries. When a geometry with smooth surfaces is used, the steady shear experiments underestimates the yield stress as revealed in Fig. 4(a). A number of researchers have observed curves similar to those in Fig. 4(a) [Buscall *et al.* (1993); Barnes (1995, 1999); Russel and Grant (2000); Roberts and Barnes (2001)]. In the case of the dynamic shear experiments [Fig. 4(b)], both the smooth and serrated geometries give the same G' value at low stresses. However, with the smooth surface, slip starts to occur at larger stress amplitudes, which is seen as a departure from the apparent linear viscoelastic (LVE) regime. After the sample begins to slip and shows an apparent yield, a ''hump'' or secondary plateau occurs. Careful analysis of a variety of slip and ''no-slip'' dynamic stress–sweep curves shows that the midpoint of this hump coincides with the yield stress estimated from the minimal-slip case of the serrated plate curve.

In Fig. 4 comparison of smooth surface geometry with roughened (serrated) geometry is used to detect wall slip. An alternate method, mentioned in Sec. I A, is to use smooth surface geometries with varying gap sizes [Yoshimura and Prud'homme (1987)]. When we used parallel plates with different gaps, we were unable to detect changes in the

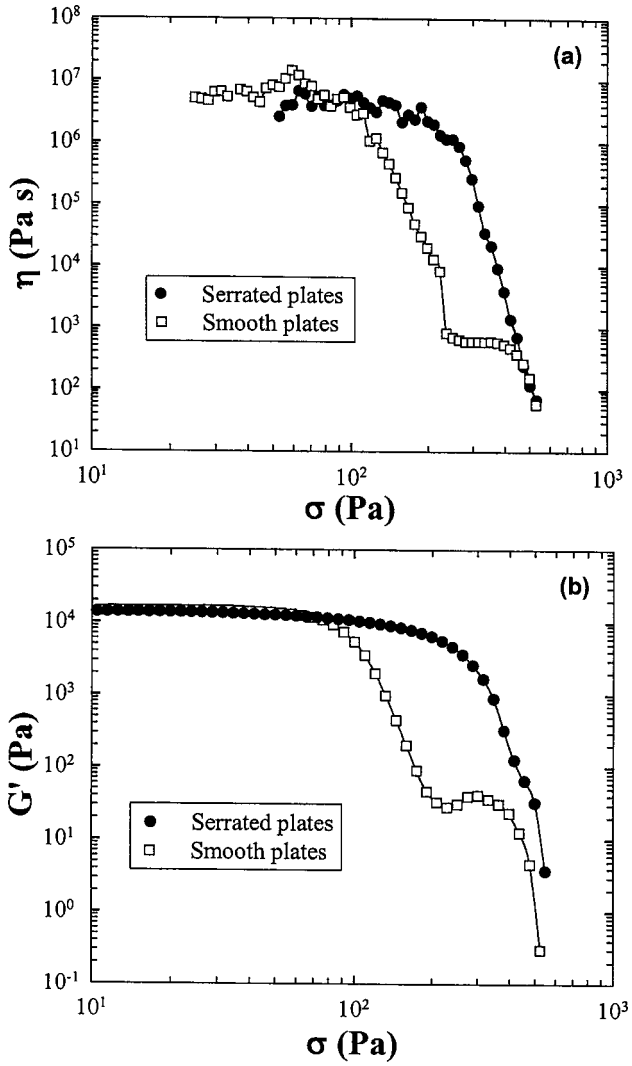

FIG. 4. Effect of the test geometry on slip for a silica gel ($\phi \sim 0.045$) containing 1.06 M LiTFSI salt. (a) Steady stress data. (b) Dynamic stress data.

observed viscosity or gel modulus outside the uncertainty in the measurement. Russel and Grant (2000) also had similar problems detecting an effect of gap on observed flow curve for their colloidal silica gels, which also exhibited wall slip. Therefore, we find comparison of geometries with smooth and roughened surfaces the simplest method of detecting the occurrence of wall slip in our colloidal silica gels.

It has been reported that the shape of the response resulting from a sinusoidal deformation can be useful in determining sample yielding and slippage [Onogi *et al.* 1970; Yoshimura and Prud'homme (1987); Hatzikiriakos and Dealy (1991); Graham (1995)]. In this regard, Hatzikiriakos and Dealy (1991) observed the appearance of higher harmonics on the stress wave forms of polymer melts and attributed this to a lack of adhesion (or debonding) of the polymer melt from the walls after the critical stress is reached. Graham (1995) showed that both viscoelasticity and dynamic slip are necessary to produce such nonsinusoidal stress in melts. Komatsu *et al.* (1973), in their experiments with commer-

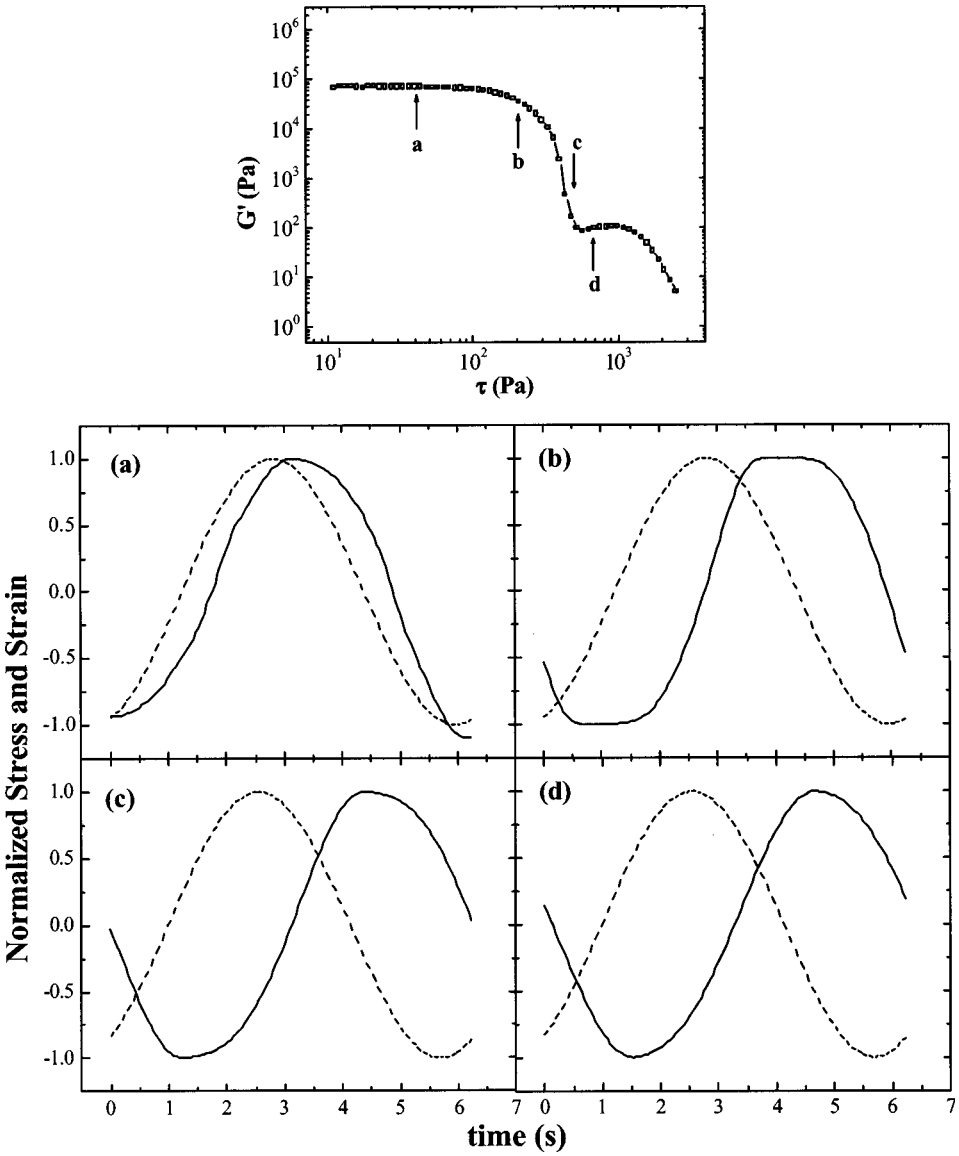

FIG. 5. Strain wave forms (solid curves) obtained with smooth plate geometry at different stress amplitudes for $\phi \sim 0.045$, 0 M samples. The stress amplitudes correspond to the values indicated in the G' vs σ plot. Dashed lines in (a)–(d) denote the stress wave forms imposed.

cial cosmetic creams, observed nonsinusoidal stresses, which they believed to be caused by dynamic yielding. For materials with yield stress, Yoshimura and Prud'homme (1987) showed that the stress wave form becomes flat beyond the occurrence of the yield stress. In order to analyze the shape of the strain waves of our system obtained with smooth geometries, we performed transient single point experiments on a representative sample containing ~ 0.045 volume fraction fumed silica and no salt (see Fig. 5) at different stress levels. Each plot (a)–(d) corresponds to a single experiment at the indicated stress amplitude shown in the top G' versus stress plot. At the low stress amplitude (point a in top figure) in the linear viscoelastic regime, the strain wave form is sinusoidal [Fig. 5(a)].

At stress amplitude (point b in top figure) where G' has deviated from its original value, the strain wave seems to flatten out considerably. For the stress level (point c in top figure) in the regime where G' is decreasing sharply, the stain wave form remains flat [Fig. 5(c)] but not to the extent observed in Fig. 5(b). Finally, the sinusoidal shape of the wave form [Fig. 5(d)] is recovered at a stress value (point d in top figure) where the secondary plateau is observed.

We conjecture from our results in Fig. 5 that both yielding and slip occur in our system with an increase in stress amplitude [Yoshimura and Prud'homme (1987); Prud'homme (2002)]. At low stresses, like in Fig. 5(a), the sample microstructure is intact and we observe a sinusoidal response. For the cases presented in Figs. 5(b) and 5(c), both yielding and slip occur. Our result in Fig. 5(b) is reminiscent of the behavior observed by Yoshimura and Prud'homme (1987) for materials with yield stress, leading us to suggest that the flat wave form is predominantly due to the microstructure being disrupted. At stresses corresponding to the second G' plateau [Fig. 5(d)], we sample material near the wall with broken/lower microstructure than the bulk. In this particle-lean slip layer, the stresses are now in the linear regime and the sinusoidal wave form is regained. At stresses corresponding to those in Fig. 5(c), the wave form is not as flat as in Fig. 5(b) and tends towards the sinusoidal profile in Fig. 5(d). In this case, slippage is dominant although there is some yielding or microstructural breakdown. It should be noted that further work needs to be undertaken to verify this hypothesis and delineate when yielding ends and/or slip starts. However, the important point to note is that the strain wave form is sinusoidal at the low G' plateau regime, indicating that we are probing material in the linear regime. Such a scenario is possible if a particle-lean slip layer exists. Our results obtained with surface modified plates (see Sec. III C) also lend credence to this notion.

Summarizing these findings, at moderately high stress amplitudes that correspond to the second G' plateau, wall slip occurs possibly due to a thin layer of particle-lean fluid near the walls deforming more than the bulk of the material. At sufficiently large stress amplitudes (beyond the second G' plateau), the fumed silica network structure throughout the entire sample is disrupted and the bulk material begins to flow and approaches the behavior observed in the minimal wall slip with the serrated plates. The reestablishment of bulk flow at large stresses is consistent with previous studies of wall slip of colloidal dispersion using steady shear [Buscall *et al.* (1993)]. An alternative explanation for the presence of two plateaus that we considered was the presence of two types of microstructures in the colloidal gels with the disruption of each structure corresponding to the catastrophic drop in G'. The presence of secondary structures has previously been observed through both microscopy and rheology in gels containing inorganic dibenzylidene sorbitol (DBS) fillers [Ilzhoefer *et al.* (1995)]. However, if such a scenario existed with fumed silica, the dual plateau and G' drop-off behavior would have remained with the use of serrated plates. The fact that both geometries provide overlapping data at low stresses is significant since it suggests that one is free to use the favored cone and plate geometry, with its uniform flow fields, to characterize the linear viscoelastic properties of a gel. Although here and elsewhere in this paper we compare slip results from cone and plate to minimal slip with parallel serrated plates, the results for smooth parallel plates exhibit similar behavior to those observed for the cone and plate.

The effect of salt concentration on slip and yield stress is examined in Fig. 6. It shows G' as a function of increasing stress amplitude for a range of salt concentrations at a constant fumed silica concentration ($\phi \sim 0.045$), using (smooth) cone and plate geometry. We find the modulus increases with the salt concentration and all samples to show two G' plateaus, indicative of the presence of wall slip. However, the secondary G' plateau (or hump) at high stress amplitude appears to decrease with an increase in salt

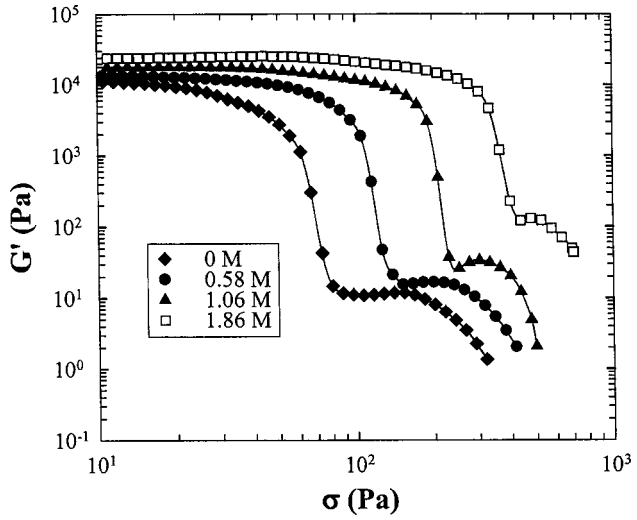

FIG. 6. Effect of salt on slip in dynamic stress data for cone and plate geometry. The volume fraction of filler in the samples was maintained at $\phi \sim 0.045$.

concentration, suggesting that increasing the salt content may decrease wall slip. Furthermore, the low stress G' plateau seems to increase with the salt concentration thereby raising the question as to whether the linear viscoelastic region increases in the presence of salt. A systematic study was therefore undertaken with both serrated plates and cone and plate geometries to address these two issues, the results of which are shown in Fig. 7.

In Fig. 7, we plot the elastic stress ($G'\gamma$) as a function of strain for various salt-containing samples using smooth and serrated geometries. In the case of serrated plates [Fig. 7(a)], a maximum in elastic stress, corresponding to the yield stress, is observed that increases with the salt concentration. Note that the maximum is broad in all cases, suggesting yielding occurs gradually, unlike in anisotropic clay systems [Walls (2002) Chap. 5]. Furthermore, yielding occurs in the same strain range regardless of the salt concentration. In the case of smooth plates [Fig. 7(b)], the presence of two maxima in the elastic stress, regardless of the salt concentration, clearly indicates slip, with the first maximum corresponding to the ''apparent'' yielding with slip. If the addition of salt, however, reduces wall slip as suggested by the smaller hump in Fig. 6, then the estimate of yield stress in the presence of slip should increase as a function of the salt. Table III gives a comparison of the yield stresses obtained with and without serrated plates. Surprisingly, underestimation of the yield stress seems to be constant at about 60% and is not a function of the salt content. The strain at yielding, vis à vis the linear viscoelastic region, also is unaffected by the presence of salt.

The next question we addressed was if the gel modulus, regardless of the matrix composition, affects wall slip. Since the gel modulus is a strong function of the fumed silica content, PEGdm 250 without salt was chosen as the matrix and dynamic stress experiments were conducted as a function of the fumed silica content using the smooth cone and plate. Figure 8 shows G' as a function of the stress amplitude for four fumed silica concentrations. The presence of slip is observed in all cases. The addition of fumed silica increases the elastic modulus and yield stress but does not seem to alter the extent of the secondary plateau or hump, in contrast to the case of an increase in salt content. In Table IV, we have quantified this wall slip effect in terms of the differences in elastic

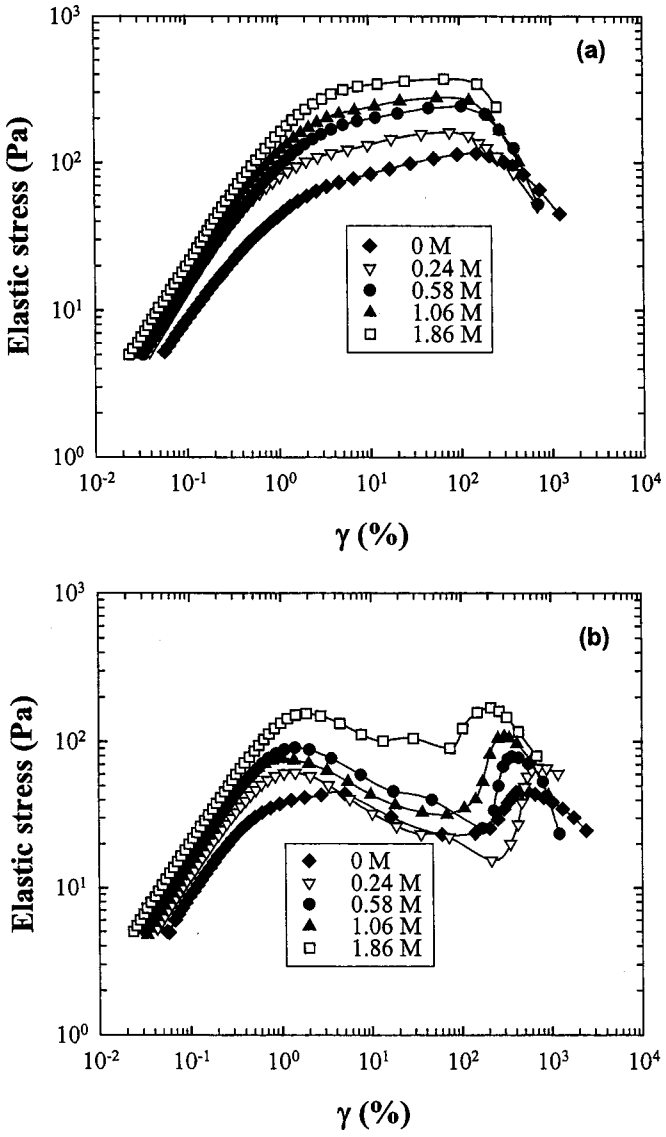

FIG. 7. Effect salt and geometry on elastic stress data for silica gels with $\phi \sim 0.045$. (a) Serrated plates. (b) Cone and plate.

TABLE III. Effect of salt on slip measured by the apparent yield stress using the elastic stress method ($\phi \sim 0.045$).

[LiTFSI] (M)	G' (Pa)	σ_y-serrated plates (Pa)	σ_y-cone and plate (Pa)	Underestimation by cone and plate (%)
0	1.09×10^4	115	44	62
0.24	1.50×10^4	160	61	62
0.58	1.56×10^4	242	91	62
1.06	1.88×10^4	276	93	66
1.86	2.18×10^4	372	154	58

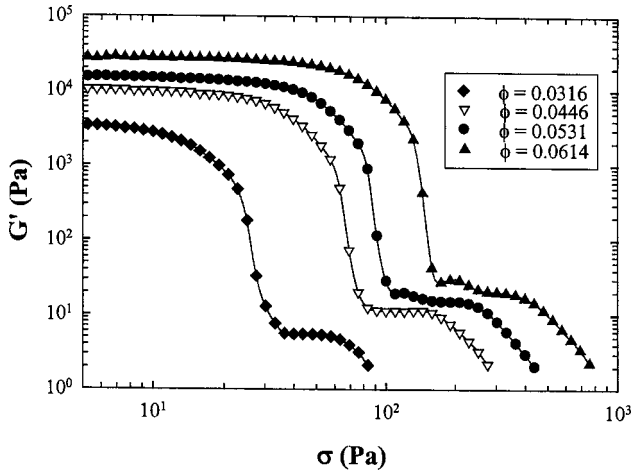

FIG. 8. Effect of the fumed silica concentration on slip in dynamic stress sweeps for cone and plate geometry. The samples contain no salt.

yield stress with and without serrated plates. There is virtually no change in the underestimation of yield stress with an increase in fumed silica; the cone and plate geometry underestimates the yield stress by about 62% in all cases. It is interesting to note that the same degree of underestimation was observed in our experiments with various amounts of salt.

Given the apparent lack of effect of the gel modulus on the secondary plateau and wall slip, we examined if the solvent medium viscosity affected yield stress and wall slip. Five different oligomers of ethylene glycol and poly(propylene glycol) were selected with the viscosities spanning two decades (see Table I). For the linear rheology of fumed silica gels in these solvents, given in detail elsewhere [Raghavan *et al.* (2000)], we find that G' scales as the mismatch in solubility parameters of the fumed silica surface and the solvating medium. Large amplitude dynamic stress experiments on these samples (Fig. 9) reveal a wide range of behavior with the occurrence of a large secondary plateau in some solvents as well as the near disappearance of it in other solvents. We have therefore compared the apparent yield stress for these samples obtained with cone and plate geometry with that using serrated parallel plate geometry to estimate the extent of slip (Table V). Unlike the salt effect, a clear trend is observed with increasing solvent viscosity and it shows a decrease in yield stress underestimation. Note also in Table V that these data support the hypotheses that the gel modulus has little effect on wall slip. Figure 10

TABLE IV. Effect of the gel modulus (due to fumed silica) on slip measured by the apparent yield stress using the elastic stress method.

ϕ	G' (Pa)	σ_y-serrated plates (Pa)	σ_y-cone and plate (Pa)	Underestimation by cone and plate (%)
0.0337	2.83×10^3	46.7	17	64
0.0447	9.59×10^3	106	40	62
0.0513	1.07×10^4	136	53	61
0.0572	1.48×10^4	175	68	61
0.0655	2.50×10^4	261	94	64

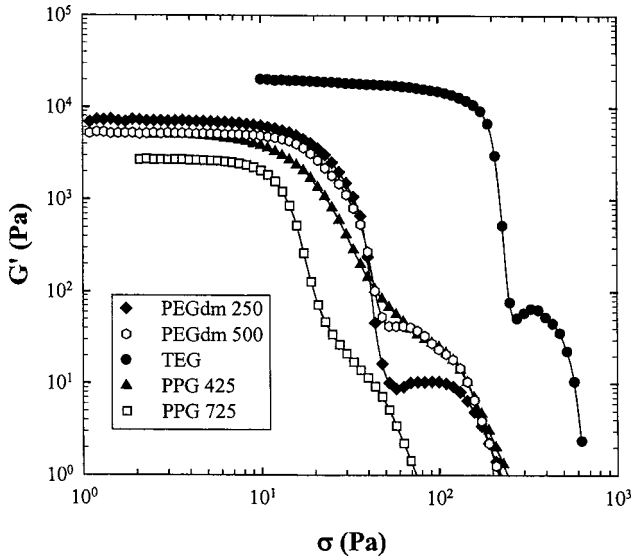

FIG. 9. Effect of the solvating medium viscosity on slip. Dynamic stress sweeps for cone and plate geometry for samples without salt and with silica volume fraction $\phi \sim 0.045$.

shows the underestimation of yield stress by the cone and plate geometry as a function of the solvent viscosity. A sigmoidal shape is observed, suggesting a transition in the effect of viscosity on slip. However, the two highest viscosities are for oligomers of different chemical structure, poly(propylene glycol) instead of poly(ethylene glycol). It is of interest to note that adding salts to polyethylene glycol also increases the solvent viscosity (Fig. 1). However, such increases in viscosity due to salt play no role in wall slip as observed in Table III.

C. Effect of surface energy on slip

In polymer melts, slip is generally believed to occur due to debonding or desorption events between the wall and the polymer. Genieser *et al.* (2000) studied the effect of different wall surface chemistries for shear stress exerted on PDMS elastomers. They compared elastomer sliding across surfaces treated with SiO_2 to surfaces treated with PDMS-OH and found that the shear stress for the SiO_2 surfaces was 10 times greater. The interaction between the wall and the sample is, therefore, very important. In colloidal gels the existence of particle-lean layers, which experience higher shear than the bulk of the

TABLE V. Effect of the solvent viscosity on slip for gels with $\phi \sim 0.045$ fumed silica and no salt.

Solvent	Viscosity (Pa s)	G' (Pa)	σ_y-serrated plates (Pa)	σ_y-cone and plate (Pa)	Underestimation by cone and plate (%)
PEGdm 250	0.0068	7.14×10^3	83	27	67
PEGdm 500	0.028	5.40×10^3	76	26	66
TEG	0.047	2.06×10^4	361	165	54
PPG 425	0.068	5.61×10^3	53	41	22
PPG 725	0.118	2.82×10^3	18	15	20

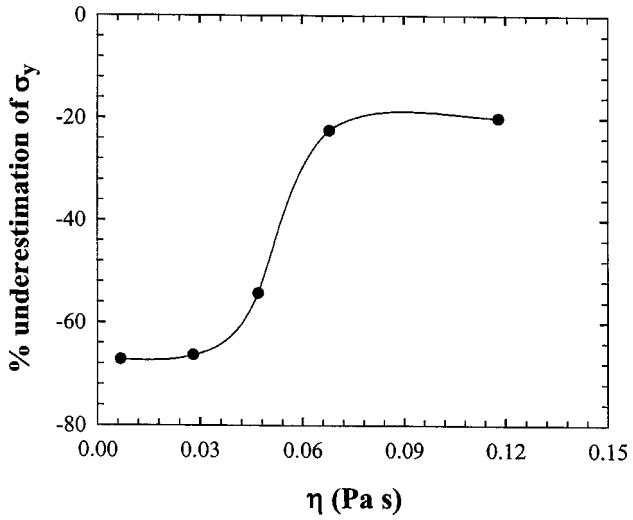

FIG. 10. Effect of the viscosity on slip. The percent of underestimation of yield stress due to slip for cone and plate geometry compared to serrated plate geometry with minimal slip. The samples are those in Fig. 9.

sample, is believed to be responsible for slip. We have attempted to change the interaction of the gel with the wall by making geometries with different surface energies.

We used parallel plates coated with Sylgard-184 PDMS to make geometries with different surface energies. Cured Sylgard-184 PDMS is hydrophobic and has a water contact angle of 109° (low surface energy). Sylgard-184-PDMS can be modified to be hydrophilic via exposure to ultraviolet and ozone [Efimenko *et al.* (2002)]. The hydrophilic plates used had a water contact angle of less than 10° (high surface energy). Figure 11 shows a comparison of dynamic stress sweeps from two different samples of 0 M gels with $\phi \sim 0.045$ for unmodified parallel plates, hydrophobic or hydrophilic parallel plates, and serrated plates (the base line, no-slip case). We find from Fig. 11(a) that the hydrophobic plates seem to reduce slip although not remove it. Interestingly, the hydrophilic plates [Fig. 11(b)] also appear to reduce slip, but to a much lesser degree than the hydrophobic plates.

Figure 12 shows the effect of the various plate surfaces on the dynamic stress behavior of an electrolyte gel with 1.86 M salt and $\phi \sim 0.045$. In this case, we observe that the hydrophobic plates [Fig. 12(a)] reduce slip significantly and produce data (e.g., $\sigma_y = 350$ Pa) comparable to those with the serrated plates (e.g., $\sigma_y = 372$ Pa). The hydrophilic plates [Fig. 12(b)] have minimal effect on slip and produce data analogous (within 10%–12%) to those obtained using smooth plates. These results can be explained based on the fact that the fumed silica particles have hydrophobic surfaces. As a result, one would expect that the particles would interact strongly with the hydrophobic test plates, thus reducing or even eliminating wall slip. On the other hand, when hydrophilic test plates are used, the wall would repel the fumed silica particles whereas the polar electrolyte would be attracted to the wall. The expected result for the hydrophilic plates would be very little change in wall slip. Our results in Fig. 12 agree well with this hypothesis, while those depicted in Fig. 11 show the correct trend, although not agreeing quantitatively. One of the interesting results in Fig. 11 is that the hydrophilic surfaces also show a decrease in wall slip. One possible explanation is that exposing the hydrophilic PDMS to gel samples results in partial disruption of the UVO created hydrophilic sur-

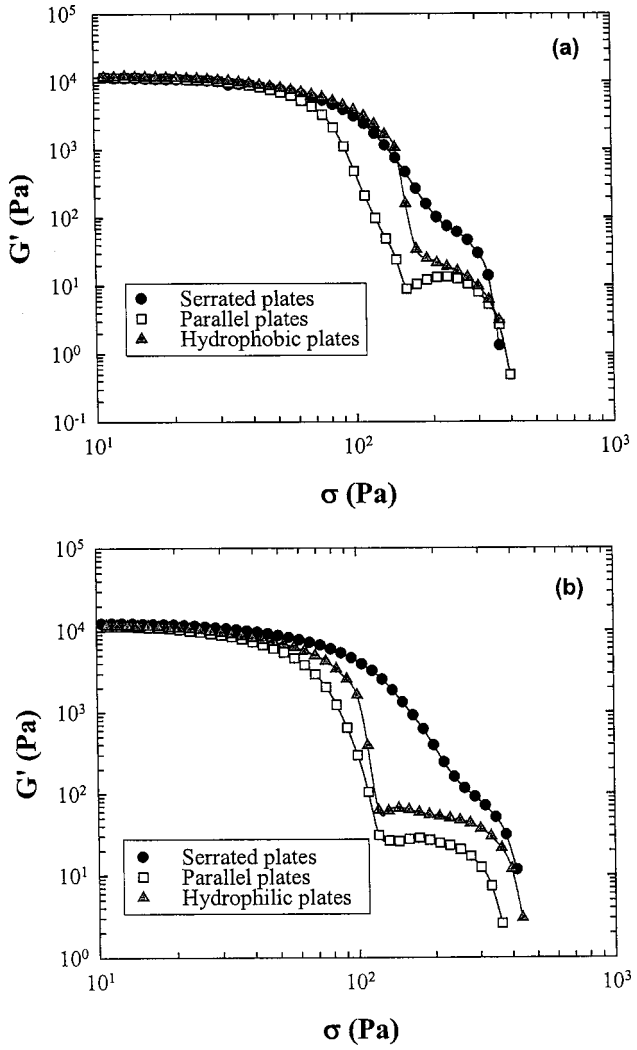

FIG. 11. Effect of the plate surface energy on slip for 0 M, $\phi \sim 0.045$ samples. (a) Comparison of slip and no-slip plates with hydrophobic parallel plates. (b) Comparison of slip and no-slip plates with hydrophilic parallel plates.

face. In other words, the surface energy of the test plates was lower during experiments than when first prepared (increase in water contact angle).

IV. SUMMARY

In this study, we compared three different measurement methods of the yield stress, in the absence of wall slip, of colloidal gels composed of oligomers of PEO, lithium salt, and hydrophobic fumed silica. The first method entails extrapolation of the steady shear stress data plotted either as a function of the apparent viscosity versus shear stress or as shear stress versus the shear rate to obtain an estimate of yield stress. The second method involves dynamic experiments as a function of increasing stress/strain amplitude. A plot of the elastic stress ($G'\gamma$) as a function of strain produces a maximum that corresponds to the yield stress. The third approach considers the stress amplitude at which G' and G''

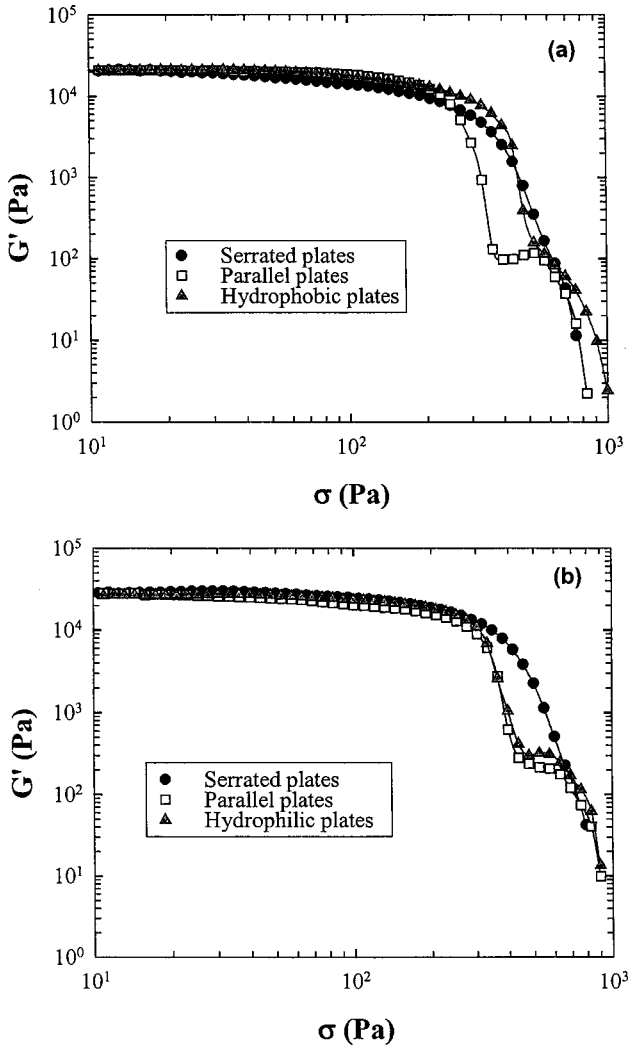

FIG. 12. Effect of the plate surface energy on slip for 1.86 M, $\phi \sim 0.045$ samples. (a) Comparison of slip and no-slip plates with hydrophobic parallel plates. (b) Comparison of slip and no-slip plates with hydrophilic parallel plates.

cross over in a dynamic stress experiment as the yield stress. We find good agreement between the steady stress experiments and the elastic stress method. However, the G', G'' crossover method consistently overestimates the yield stress by approximately 40%.

Experiments conducted with smooth surface geometries, however, reveal the presence of slip in the colloidal gels and yielding at much lower stresses. Neither increasing the fumed silica content nor adding salt affects this slip behavior. However, higher viscosity of the solvating medium appears to reduce the occurrence of wall slip. An attempt at influencing the formation of the slip layer was made by using test geometries with hydrophobic and hydrophilic surface chemistries. The hydrophilic surface had minimal effect on slip. However, the hydrophobic surface reduces slip, possibly due to the improved interactions of the hydrophobic fumed silica with the wall.

ACKNOWLEDGMENTS

The authors gratefully acknowledge the funding of this study by the Department of Energy, Office of Basic Energy Sciences, and the Office of Transportation Technology through Lawrence Berkeley National Laboratories. The generosity of Degussa Corporation and 3M Company for providing R805 fumed silica and the LiTFSI salt, respectively, is much appreciated. They are indebted to Dr. Kirill Efimenko (NC State University) for making the PDMS films and to Professor Robert Prud'homme (Princeton University), Professor Jan Genzer (NC State University), and Professor Srinivasa Raghavan (University of Maryland) for many fruitful discussions.

References

Anastasiadis, S. H., and S. G. Hatzikiriakos, ''The work of adhesion of polymer/wall interfaces and its association with the onset of wall slip,'' J. Rheol. **42**, 795–812 (1998).

Aral, B. K., and D. M. Kalyon, ''Effects of temperature and surface roughness on time-dependent development of wall slip in steady torsional flow of concentrated suspensions,'' J. Rheol. **38**, 957–972 (1994).

Barnes, H. A., ''A review of the slip (wall depletion) of polymer solutions, emulsions and particle suspensions in viscometers: Its cause, character and cure,'' J. Non-Newtonian Fluid Mech. **56**, 221–251 (1995).

Barnes, H. A., ''The yield stress, a review or, everything flows?'' J. Non-Newtonian Fluid Mech. **81**, 133–178 (1999).

Barnes, H. A., and Q. D. Nguyen, ''Rotating vane rheometry—A review,'' J. Non-Newtonian Fluid Mech. **98**, 1–14 (2001).

Buscall, R., I. J. McGowan, and A. J. Morton-Jones, ''The rheology of concentrated dispersions of weakly attracting colloidal particles with and without wall slip,'' J. Rheol. **37**, 621–641 (1993).

Dimonte, G., D. Nelson, S. Weaver, and M. Schneider, ''Comparative study of viscoelastic properties using virgin yogurt,'' J. Rheol. **42**, 727–742 (1998).

Efimenko, K., W. E. Wallace, and J. Genzer, ''Surface modification of Sylgard-184 PDMS networks by ultraviolet and ultraviolet/ozone treatment,'' J. Colloid Interface Sci. **254**, 306–315 (2002).

Evans, I. D., ''On the nature of the yield stress,'' J. Rheol. **36**, 1313–1316 (1992).

Fan, J., S. R. Raghavan, X.-Y. Yu, S. A. Khan, J. Hou, and G. L. Baker, ''Composite polymer electrolytes using surface-modified fumed silica: conductivity and rheology,'' Solid State Ionics **111**, 117–123 (1998).

Genieser, L. H., K. C. P. Hendriks, F. T. P. Baaijens, and H. E. H. Meijer, ''Characterization of elastomer sliding behavior across silica and PDMS grafted surfaces,'' J. Rheol. **44**, 1003–1017 (2000).

Gevgilili, H., and D. M. Kalyon, ''Step strain flow: Wall slip effects and other error sources,'' J. Rheol. **45**, 467–475 (2001).

Graham, M. D., ''Wall slip and the nonlinear dynamics of a large amplitude oscillatory shear flows,'' J. Rheol. **39**, 696–712 (1995).

Gray, F. M., *Polymer Electrolytes* (Royal Society of Chemistry, Cambridge, 1997).

Hatzikiriakos, S. G., and J. M. Dealy, ''Wall slip of molten high density polyethylene. I. Sliding plate rheometer studies,'' J. Rheol. **34**, 497–523 (1991).

Husband, D. M., and N. Aksel, ''The existence of static yield stresses in suspensions containing noncolloidal particles,'' J. Rheol. **37**, 215–235 (1993).

Ilzhoefer, J. R., B. C. Broom, S. M. Nepa, E. A. Vogler, S. A. Khan, and R. J. Spontak, ''Evidence of hierarchical order in an amphilphili graft terpolymer gel,'' J. Phys. Chem. **99**, 12069–12071 (1995).

Joshi, Y. M., A. K. Lele, and R. A. Mashelkar, ''A unified wall slip model,'' J. Non-Newtonian Fluid Mech. **94**, 135–149 (2000).

Khan, S. A., and N. J. Zoeller, ''Dynamic rheological behavior of flocculated fumed silica suspensions,'' J. Rheol. **37**, 1225–1235 (1993).

Komatsu, H., T. Mitsui, and S. Onogi, ''Nonlinear viscoelastic properties of semisolid emulsions,'' Trans. Soc. Rheol. **17**, 351–364 (1973).

Leger, L., H. Hervet, G. Massey, and E. Durliat, ''Wall slip in polymer melts,'' J. Phys.: Condens. Matter **9**, 7719–7740 (1997).

Macosko, C. W., *Rheology: Principles, Measurements, and Applications* (VCH, New York, 1994).

Nguyen, Q. D., and D. V. Boger, ''Yield stress measurement for concentrated suspensions,'' J. Rheol. **27**, 321–349 (1983).

Nguyen, Q. D., and D. V. Boger, ''Measuring the flow properties of yield stress fluids,'' Annu. Rev. Fluid Mech. **24**, 47–88 (1992).

Onogi, S., T. Masuda, and T. Matsumoto, ''Non-linear behavior of viscoelastic materials. I. Disperse systems of polystyrene solution and carbon black,'' Trans. Soc. Rheol. **14**, 275–294 (1970).

Pai, V. B. and S. A. Khan, ''Gelation and rheology of xanthan/enzyme-modified guar blends,'' Carbohydr. Polym. **49**, 207–216 (2002).

Prud'homme, R. K. (personal comunications, 2002).

Raghavan, S. R., ''Suspensions, gels, and composite electrolytes based on—fumed silica: Rheology and microstructure,'' Ph.D. thesis, North Carolina State University, Raleigh, NC, 1998.

Raghavan, S. R., and S. A. Khan, ''Shear-induced microstructural changes in flocculated suspensions of fumed silica,'' J. Rheol. **39**, 1311–1325 (1995).

Raghavan, S. R., J. Hou, G. L. Baker, and S. A. Khan, ''Colloidal interaction between particles with tethered nonpolar chains dispersed in polar media: Direct correlation between dynamic rheology and interaction parameters,'' Langmuir **16**, 1066–1077 (2000).

Raghavan, S. R., M. W. Riley, P. S. Fedkiw, and S. A. Khan, ''Composite polymer electrolytes based on poly(ethylene glycol) and hydrophobic fumed silica: Dynamic rheology and microstructure,'' Chem. Mater. **10**, 244–251 (1998).

Roberts, G. P., and H. A. Barnes, ''New measurements of the flow curves for carbopol dispersions without slip artifacts,'' Rheol. Acta **40**, 499–503 (2001).

Russel, W. B., and M. C. Grant, ''Distinguishing between dynamic yielding and wall slip in a weakly flocculated colloidal dispersion,'' Colloids Surf., A **161**, 271–282 (2000).

Shi, J., and C. A. Vincent, ''The effect of molecular weight on cation mobility in polymer electrolytes,'' Solid State Ionics **60**, 11–17 (1993).

Shih, W. Y., W.-H. Shih, and I. A. Aksay, ''Elastic and yield behavior of strongly flocculated colloids,'' J. Am. Ceram. Soc. **82**, 616–624 (1999).

Soltani, F., and U. Yilmazer, ''Slip velocity and slip layer thickness in flow of concentrated suspensions,'' J. Appl. Polym. Sci. **70**, 515–522 (1998).

Walls, H. J., ''Colloidal silica gels as composite electrolytes: Rheology and ion transport,'' Ph.D. thesis, North Carolina State University, Raleigh, NC, 2002.

Walls, H. J., J. Zhou, J. A. Yerian, P. S. Fedkiw, S. A. Khan, M. K. Stowe, and G. L. Baker, ''Fumed silica-based composite polymer electrolytes: Synthesis, rheology, and electrochemistry,'' J. Power Sources **89**, 156–162 (2000).

Yang, M. C., L. E. Scriven, and C. W. Macosko, ''Some rheological measurements on magnetic iron oxide suspensions in silicone oil,'' J. Rheol. **30**, 1015–1029 (1986).

Yoshimura, A. S., and R. K. Prud'homme, ''Response of an elastic Bingham fluid to oscillatory shear,'' Rheol. Acta **26**, 428–436 (1987).

Yoshimura, A. S., R. K. Prud'homme, H. M. Princen, and A. D. Kiss, ''A comparison of techniques for measuring yield stresses,'' J. Rheol. **31**, 699–710 (1987).

Yziquel, F., P. J. Carreau, and P. A. Tanguy, ''Non-linear viscoelastic behavior of fumed silica suspensions,'' Rheol. Acta **38**, 14–25 (1999).